



Cardiac Regeneration by Statin-Polymer Nanoparticle-Loaded Adipose-Derived Stem Cell Therapy in Myocardial Infarction

RYO YOKOYAMA,^a MASAOKI I^b,^{ORCID} MISAOKI MASUDA,^b YASUHIKO TABATA,^c MASAOKI HOSHIGA,^a NOBUKAZU ISHIZAKA,^a MICHIO ASAHI^d

Key Words. Adipose stem cells • Cardiac • Stem cell transplantation • Tissue regeneration

^aDepartment of Cardiology, Faculty of Medicine, Osaka Medical College, Osaka, Japan; ^bDivision of Research Animal Laboratory and Translational Medicine, Research and Development Center, Osaka Medical College, Osaka, Japan; ^cLaboratory of Biomaterials, Institute for Frontier Life and Medical Sciences, Kyoto University, Kyoto, Japan; ^dDepartment of Pharmacology, Faculty of Medicine, Osaka Medical College, Osaka, Japan

Correspondence: Masaaki Ii, M.D., Ph.D., Division of Research Animal Laboratory and Translational Medicine, Research and Development Center, Osaka Medical College, 2-7, Takatsuki, Osaka 569-8686, Japan. Telephone: 81-72-684-6537; e-mail: masaii@osaka-med.ac.jp

Received October 28, 2018; accepted for publication April 20, 2019; first published June 3, 2019.

<http://dx.doi.org/10.1002/sctm.18-0244>

This is an open access article under the terms of the Creative Commons Attribution-NonCommercial-NoDeriv License, which permits use and distribution in any medium, provided the original work is properly cited, the use is non-commercial and no modifications or adaptations are made.

ABSTRACT

Clinical trials with autologous adipose-derived stem cell (AdSC) therapy for ischemic heart diseases (IHDs) are ongoing. However, little is known about combinational therapeutic effect of AdSCs and statin poly(lactic-co-glycolic) acid (PLGA) nanoparticles on the ischemic myocardium. We investigated the hypothesis that statins, which have pleiotropic effects, augment the therapeutic potential of AdSCs and that AdSCs also act as drug delivery tools. Simvastatin-conjugated nanoparticles (SimNPs) significantly promoted migration activity without changing proliferation activity and upregulated growth factor gene expression *in vitro*. A small number of intravenously administered SimNP-loaded AdSCs (10,000 cells per mouse) improved cardiac function following myocardial infarction, inducing endogenous cardiac regeneration in the infarcted myocardium. The *de novo* regenerated myocardium was thought to be derived from epicardial cells, which were positive for Wilms' tumor protein 1 expression. These findings were attributed to the sustained, local simvastatin release from the recruited SimNP-loaded AdSCs in the infarcted myocardium rather than to the direct contribution of recruited AdSCs to tissue regeneration. SimNP-loaded AdSCs may lead to a novel somatic stem cell therapy for IHDs. *STEM CELLS TRANSLATIONAL MEDICINE* 2019;8:1055–1067

SIGNIFICANCE STATEMENT

Damaged myocardium is known for inability to regenerate, as is also true for damaged brain/spinal cord. The present study showed that only a single administration of a small number of simvastatin-conjugated polymer nanoparticles loaded adipose-derived stem cells induced spontaneous cardiac regeneration in infarcted myocardium, exhibiting the recovery of impaired cardiac function. In most cases of stem cell therapy for myocardial infarction, the therapeutic effect is attributed to the reduction of myocardial necrosis following ischemic injury; however, the technique we developed successfully induced myocardial regeneration with increased vascularity and pericardium-derived *de novo* cardiomyocytes. These findings may give rise to an innovative therapy of myocardial infarction without using ES cell- or iPS cell-derived cardiomyocytes.

INTRODUCTION

Cardiovascular disease has been recognized as one of the major causes of death, and numerous patients suffer from heart failure, which is a leading cause for hospitalization worldwide [1]. Despite a variety of therapeutic options for preventing cardiovascular disease-induced heart failure, patients are often being treated with invasive cardiac surgery even at the end stage, including heart transplantation. In animal models of myocardial infarction (MI) and in early-phase clinical trials, bone marrow (BM)-derived stem/progenitor cell transplantation has recently been

reported to be effective as a new therapeutic strategy for promoting cardiomyogenesis and vasculogenesis in severe cardiovascular diseases. Among the variety of somatic stem cell candidates, that is, BM-/granulocyte-colony stimulating factor (G-CSF)-mobilized peripheral blood-derived endothelial progenitor cells (EPCs, CD34⁺ cells) [2], umbilical cord blood-derived stem cells (CD133⁺ cells) [3], and amnion-derived stem cells (mesenchymal stem cells, MSCs) [4, 5], which have been studied for cardiac regenerative medicine, adipose-derived mesenchymal stem cells (AdSCs) are advantageous for therapeutic

use not only because of their plasticity but also because a sufficient number of AdSCs can be easily collected by minimally invasive surgical techniques [6, 7]. AdSCs may have cardiac regenerative potential with their capability to differentiate into cardiomyocytes (CMs) *in vitro* [8–10], and their ability to secrete angiogenic and antiapoptotic factors [11] may play a therapeutic role in the ischemic myocardium. Moreover, AdSCs have been reported to accumulate in the MI area, and thus, AdSCs are expected to serve as a cell source for cardiac regeneration [11]. However, the optimal therapeutic efficacy of AdSCs on ischemic heart diseases (IHDs) has been hindered by their poor survival and low differentiation rates of these cells *in vivo* [12]. Thus, a number of studies focused on improving the survival or differentiation rate of AdSCs into cardiovascular cells have been performed. Previous studies have indicated that ameliorating the cardiac milieu after an acute MI is crucial for the viability of transplanted AdSCs [13] and that directing AdSCs can facilitate their transdifferentiation potential *in vivo* [14]. Recently, we developed a novel controlled-release drug-conjugated nanoparticle that is formulated from the bioabsorbable PLGA polymer with hydrophobic drugs, and these nanoparticles were taken up by a variety of cells such as monocytes, vascular smooth muscle cells (VSMCs), and endothelial cells (ECs) [15]. In addition, compared with conventional drug delivery systems (DDSs), this nanoparticle-mediated DDS significantly increased the therapeutic effects of ischemia-induced neovascularization in animal models [16]. Statins, a class of hydroxymethylglutaryl-coenzyme A reductase inhibitors, exhibit multiple biological activities such as promoting endothelial function, suppressing inflammation, stabilizing atherosclerotic plaques, reducing harmful oxidants, and, specifically, recruiting circulating EPCs for angiogenesis that are independent of their serum cholesterol-lowering effect [17, 18]. Therefore, we tested the hypothesis that AdSCs loaded with statin-conjugated PLGA nanoparticles exhibited a synergistic favorable effect on acute MI by promoting AdSC differentiation into cardiovascular cells and other biological effects. In this study, the combinational therapeutic effect of AdSCs and statin PLGA nanoparticles on the ischemic myocardium following MI was examined by histological and functional assessments in a mouse MI model.

MATERIALS AND METHODS

Adipose Tissue Harvesting and AdSC Isolation

Institutional Animal Care and Use Committee in Osaka Medical College approved all the following research protocols, including the surgical procedures and animal care. Human adipose-derived stem cells (hAdSCs) were isolated from the adipose tissue of adult patients, who gave informed consent, as surgical scraps from the surgical specimens of various surgeries. AdSCs were isolated from the adipose tissue as previously described with minor modifications [19]. Briefly, the adipose tissue was washed in phosphate buffered solution (PBS) and minced, followed by digestion in 5 ml of type I collagenase (1 mg/ml in 1% bovine serum albumin BSA/Hanks' balanced saline solution; Life Technologies Japan, Tokyo, Japan) for 30 minutes at 37°C with a rotator (Miltenyi Biotec K.K., Tokyo, Japan) according to the manufacturer's

instructions. The digested tissue was filtered through a 40- μ m cell strainer (BD Falcon, Tokyo, Japan) and centrifuged at 450g for 10 minutes. The cell pellet was suspended in 10% fetal bovine serum (FBS)/Dulbecco's modified Eagle medium (DMEM)/F12 medium and plated on culture dishes at 1,000–3,000 cells per cm^2 . After reaching 70% confluence, the attached cells were dissociated (0.25% trypsin EDTA; Invitrogen, Tokyo, Japan) and passaged as hAdSCs. The hAdSCs were used between the third and sixth passage in this study.

Cell Function Assay

The proliferation activity of hAdSCs was examined using a Cell Counting Kit-8 (Dojindo Laboratories, Kumamoto, Japan) according to the manufacturer's instructions. Briefly, hAdSCs were seeded onto 96-well culture plates at a density of 5×10^3 cells per well and were cultured in DMEM containing 10% FBS for 48 hours at 37°C with simvastatin-conjugated nanoparticles (SimNPs; 20 μ g/ml, 50 μ g/ml, 100 μ g/ml). The optical density at the 450-nm wavelength was measured using a plate reader. The migration activity of hAdSCs was evaluated with a modified Boyden's chamber method as described previously [20]. Briefly, hAdSCs (5×10^4 cells per well) were seeded into the upper chambers of 24-well culture plates and the lower chambers were filled with DMEM/F12 medium containing 20% FBS with SimNPs (20 μ g/ml, 50 μ g/ml, 100 μ g/ml), followed by incubation for 6 hours at 37°C. The migrated cells were stained with 4',6-diamidino-2-phenylindole (DAPI) and counted in four randomly selected high-power fields (HPFs; $\times 200$, 0.15 mm^2 per HPF) per chamber under a fluorescence microscope' and the resulting numbers were averaged.

Fluorescence Immunocytochemistry for AdSC Differentiation Assays

The attached cells were fixed with 2% paraformaldehyde (PFA)/PBS for 10 minutes at RT followed by washing in PBS and were permeabilized by incubating with 0.1% Triton X-100/PBS solution for 5 minutes at RT. The samples were blocked in 2% BSA/PBS antibody dilution buffer for 1 hour at RT. After removing the blocking solution, the following primary antibodies/markers were added in antibody dilution buffer and incubated at 4°C overnight: anti-CD31 (1:100; Abcam, Cambridge, MA) and fluorescein-Griffonia simplicifolia lectin 1, and ILB4 (Vector Laboratories, Burlingame, CA) were used for ECs; anti-SM22 (1:100; Abcam) and anti-Calponin (1:200; Abcam) antibodies were used to identify VSMCs; and GATA4 (Santa Cruz Biotechnology, Santa Cruz, CA) and cardiac Troponin T (Thermo Fisher Scientific, Fremont, CA) indicated CMs. After washing with PBS, the cells were incubated for 30 minutes at RT with the following secondary antibodies prepared at a 1:500 dilution in antibody dilution buffer: Alexa 488 donkey anti-goat IgG, Alexa 488 goat anti-rabbit IgG, and Alexa 488 goat anti-rat IgG (Jackson ImmunoResearch Laboratories, Inc., West Grove, PA). After the secondary antibodies were removed and the cells were washed with PBS, nuclear counterstaining was performed by incubating the cells with DAPI solution (Sigma-Aldrich Japan K.K., Tokyo, Japan, 1 μ g/ml in PBS) for 10 minutes at RT. The sample slides were covered by a coverslip and with mounting medium (ImmunoBioScience, Mukilteo, WA) followed by sealing with nail varnish before being evaluated under a fluorescence microscope. The antigen (marker for differentiation)-positive cells in each chamber were counted in five

different HPFs (200×) and the differentiation activity was evaluated by the percentage of antigen-positive cells to the total number of DAPI-positive cells.

Quantitative Real-Time Reverse Transcription Polymerase Chain Reaction (RT-PCR)

The hAdSCs were seeded onto 6-well culture plates and cultivated for 24 hours at 37°C in DMEM containing 10% FBS medium with SimNPs (20 µg/ml, 50 µg/ml, 100 µg/ml). Cells were harvested; RNA was extracted with an RNeasy Mini kit (Qiagen, Tokyo, Japan); cDNA was synthesized using an ExScript RT kit (Takara, Siga, Japan); and amplification was performed on a Sequence Detection System 7000 (Applied Biosystem, Tokyo, Japan) according to the manufacturer's instructions. The primer sequences and GenBank accession numbers are as follows: vascular endothelial growth factor (VEGF, AB021221), forward TCTCCCTGATCGGTGACAGT and reverse GGGCAGAGCTGAGTGTAGC; basic fibroblast growth factor (bFGF, J04513), forward CTCAGTCGGAAC AAATTGGAA and reverse GCCTGTCAGAGCTGAAGAA; insulin-like growth factor-1 (IGF-1, X00173), forward CCATGTCCTCCTCGCATCTC and reverse CGTGGCAGAGCTGGTGAAG; angiopoietin-1 (Ang-1, D13628), forward GTTGGCAAGGTAGCAATACCA and reverse GCATAGTGGATCAAGTCACCAA; stromal cell-derived factor-1 (L36033), forward TGAGAGCT CGCTTGAGTGA and reverse GCCTCCATGGCATAACATA GG; and glyceraldehyde-3-phosphate dehydrogenase (GAPDH, AF261085), forward CAGCCTCAAGATCATCAGCA and reverse TGTGGTCATGAGTCTTCCA. The relative target gene mRNA expression was calculated with the comparative CT method. The amount of the target gene was normalized to that of the endogenous GAPDH control gene. The experiments were repeated in triplicate and the results were averaged.

Animals and Experimental Groups

Male nude mice (BALB/c nu/nu; CLEA Japan) aged 12 weeks were used in this study. For assessment of cardiac function by echo cardiography and histology, mice were assigned in the following groups ($n = 8$ in each group): the (a) PBS (control) group, (b) SimNP group, (c) NP-AdSC group, and (d) SimNP-AdSC group. The mice were euthanized for harvesting hearts at 28 days after MI induction. In control group, 100 µl of PBS was injected into the tail vein. In NP-AdSC group, nanoparticle (NP, 50 µg) loaded hAdSCs (1×10^4 /100 µl of PBS) were injected into the tail vein. In SimNP group, SimNP (50 µg) were injected into the tail vein. In SimNP-AdSC group, SimNP (50 µg) loaded AdSCs (1×10^4 /100 µl of PBS) were injected into the tail vein. All the four treatments were performed on day 3 following MI induction.

Since Wilms' tumor protein 1 (WT1)-positive cells were generally able to be detected only on day 3–5 following MI in ischemic myocardium, the mice were assigned in the above same four groups ($n = 3$ in each group) and were euthanized at 14 days after MI induction for sustained appearance of WT1-positive cells in ischemic myocardium by SimNP-AdSC administration. For assessment for final cardiac tissue regeneration following MI, the mice were assigned in the above same four groups ($n = 3$ in each group) and were euthanized at 56 days after MI induction.

Surgical Procedure

Male 12- to 16-week-old nude mice (BALB/c nu/nu; CLEA Japan) were anesthetized with intraperitoneal injections of 400 mg/kg 2,2,2-tribromoethanol (Avertin, Sigma–Aldrich Japan K.K., Tokyo, Japan). MI was induced by ligating the left anterior descending (LAD) coronary artery as described previously [20, 21]. Briefly, after the fourth to fifth intercostal space was opened, the heart was exteriorized and the pericardium was incised. Thereafter, the heart was held with the forceps, and MI was induced by ligating the LAD coronary artery with a 7-0 nylon suture precisely at the proximal site of the bifurcation of the diagonal branch. The predetermined hAdSCs (hAdSC-treated group) or control dose was transplanted 3 days after the MI induction.

Physiological Assessment of Left Ventricular Function

Cardiac function in the left ventricle (LV) was sequentially evaluated by echocardiography (Nemio 30, Toshiba Medical Systems, Tochigi, Japan) via changes in ejection fraction (Δ EF), fractional shortening (Δ FS), left ventricular end-systolic dimension (Δ LVDS), and left ventricular end-diastolic dimension (Δ LVDD) before MI induction and at 1 day and 2, 4, and 12 weeks afterward. The mice were sacrificed 4 weeks after MI surgery and the hearts were harvested for histological analysis. All procedures and analyses were performed by an experienced researcher who was blinded to the treatment assignments.

Histological Analysis

The hearts were removed from the euthanized animals 28 days after the MI and were retrogradely perfused with PBS, followed by 4% PFA through the right carotid artery. The hearts were fixed for 6 hours in 4% PFA and incubated overnight in a 15% sucrose solution. The tissues were embedded in OCT compound (Sakura FineTek, Japan) and sectioned at a 1 mm thickness for rats and at 0.5 mm thickness for mice, just below the LAD ligation level at 5 mm thickness as described previously. Masson's trichrome staining was performed to evaluate fibrotic sites. The extent of MI size was evaluated by calculating (a) the percentage of the entire cross-sectional LV area that was fibrotic, (b) the percentage of the fibrosis length out of the entire cross-sectional LV circumference, and (c) the percentage of the wall thickness out of the intact cross-sectional LV wall thickness using the NIH ImageJ 1.42 software and the Adobe Photoshop CS4 (Adobe Systems, San Jose, CA) software.

Immunohistochemistry

The MI-induced mouse hearts were harvested at predetermined time points after surgery and prepared for frozen tissue sectioning after fixation with 4% PFA/PBS. Double fluorescent immunostaining was performed to detect the transdifferentiation of the transplanted hAdSCs into ECs, with an antibody against human mitochondria antigen (hMitC, Abcam), into VSMCs, with antibodies against ILB4 (Vector Laboratories) and smooth muscle α -actin (Dako), or into CMs, with antibodies against cardiac troponin-I (Abcam), Nkx2.5, α MHC, and Gata4 (Abcam). Normal mouse IgG or PBS served as negative controls. The EC marker (biotinylated) ILB4 (1:100; Vector Laboratories) was used for capillary staining with a FITC-conjugated streptavidin-biotin binding method in mouse hearts. Antibodies against Ki67 (Abcam) and WT1 (Santa Cruz Biotechnology) were used as a marker for

proliferating cells and embryogenesis-related proteins, respectively. Nuclei were counterstained with DAPI (Sigma), and sections were mounted in aqueous mounting medium. Images were examined using a fluorescence microscope (BZ-X700, Keyence, Osaka, Japan). The number of ILB4-positive capillaries within an HPF ($\times 200$) of the bilateral peri-infarct area was counted and averaged for the assessment of capillary density.

Statistical Analysis

All values are expressed as the mean \pm SEM. Statistical analyses were performed using the Prism software program (GraphPad Software, CA). Nonparametric unpaired *t* tests (Mann–Whitney *U* test) were used for comparisons between two groups and repeated-measure two-way ANOVA with Bonferroni post hoc tests were used for comparing multiple groups. *p* values $< .05$ were considered statistically significant.

RESULTS

Proliferation and Migration Activities of hAdSCs and PLGA Nanoparticles Uptake in AdSCs

To clarify the advantage of the nanoparticle-mediated DDS with AdSCs, the cellular uptake and kinetics of the PLGA nanoparticles (NPs) were examined in cultured AdSCs. The cells were seeded in a 6-well culture dish and rhodamine-conjugated PLGA-NPs were added to the dish at different doses. After 1 or 2 hours of incubation, the extracellular rhodamine-conjugated NPs were washed out and the AdSCs were observed under a confocal laser microscope. AdSCs internalized PLGA-NPs after 1- and 2-hour incubations in culture, and the NPs were observed around the nuclei, indicating that the NPs were distributed in the cytosol (Fig. 1A). Analysis of the *in vitro* statin release kinetics of the PLGA-NPs from AdSCs revealed an early burst of statin release, approximately 50% of the total simvastatin PLGA-NP uptake, on day 1, followed by the sustained release of the remaining PLGA-NPs for up to 2 weeks (Fig. 1B). The migration activity of the cells treated with the different concentrations of PLGA-NP ($50 \mu\text{g}/5 \times 10^4$ cells) or simvastatin NP (SimNP)-loaded AdSCs were evaluated using a Transwell culture plate, and the number of AdSCs that migrated toward the 20% fetal bovine serum (FBS) was determined as the migration activity. The AdSCs loaded with $50 \mu\text{g}$ of SimNPs/ 5×10^4 cells presented with significantly increased migration activity, whereas those loaded with $100 \mu\text{g}$ of SimNPs/ 5×10^4 cells had inhibited migration (Fig. 1C). The proliferation activity of the AdSCs loaded with different concentrations of PLGA NPs or SimNPs was evaluated as the mean optical density value at a wavelength of 450 nm after 48 hours in culture. Although the proliferation activity of AdSCs loaded with $100 \mu\text{g}$ of SimNPs/ 5×10^4 cells was significantly reduced, when the control group was compared with the other groups with AdSCs loaded with different SimNP concentrations, no significant change in proliferation activity was observed (Fig. 1D).

Simvastatin-Conjugated PLGA NPs Increased Growth Factor Gene Expression in AdSCs

Growth factor/cytokine production in AdSCs was evaluated as mRNA expression with quantitative real-time RT-PCR. VEGF A mRNA expression in AdSCs was significantly upregulated with the SimNP treatment, peaking at the concentration of

$20 \mu\text{g}/5 \times 10^4$ cells (Fig. 1E). VEGF C mRNA expression in AdSCs was significantly upregulated, peaking at an SimNP concentration of $100 \mu\text{g}/5 \times 10^4$ cells (Fig. 1F) FGF2, Angiopoetin1, and IGF-1 mRNA expression levels in AdSCs were significantly upregulated with the SimNP treatment, peaking at the $50 \mu\text{g}/5 \times 10^4$ cells concentration (Fig. 1G–1I). These results suggest that AdSCs have the ability to produce pro-angiogenic cytokines such as VEGF, FGF2, and Angiopoetin1 and to regulate the antiapoptotic growth factor IGF-1 in the acute phase following MI to promote neovascularization and inhibit cardiovascular cell death.

Simvastatin-Conjugated NP-Loaded AdSCs Exhibit High Differentiation Capacity for Vascular Cells

Next, we assessed the transdifferentiation capacity of AdSCs with or without SimNPs using the markers Calponin/ $\text{SM}\alpha$ -actin for VSMCs and Isolectin B4 (ILB4)/CD31 for ECs. SMC differentiation medium significantly increased the percentage of Calponin/ $\text{SM}\alpha$ -actin-positive cells, and SimNP uptake further significantly increased this percentage (Fig. 2A, 2C). EC differentiation medium also significantly increased the percentage of ILB4/CD31-positive cells, and SimNP uptake further significantly increased this percentage (Fig. 2B, 2D). However, under regular culture conditions, only a small population of AdSCs faintly expressed Calponin/ $\text{SM}\alpha$ -actin, and these cells did not express ILB4/CD31. These results suggest that SimNP uptake enhanced the smooth muscle and endothelial differentiation of AdSCs under each differentiation condition.

SimNP-AdSC Transplantation Improved Cardiac Functional Recovery Following MI

Echocardiography assessment at 14 and 28 days after cell transplantation revealed that the left ventricular (LV) ejection fraction/LV fractional shortening parameters, which directly indicate LV contractile function, were significantly increased in the SimNP-AdSC-treated group than in the control-, NP-AdSC-, and SimNP-treated groups (Fig. 3A, 3B), and the left ventricular dimension in diastole (LVDd)/left ventricular dimension in systole (LVDs) parameters, which indirectly indicate LV function, were significantly increased in the SimNP-AdSC-treated group than in the control-, NP-AdSC-, and SimNP-treated groups (Fig. 3C, 3D). Next, we histologically assessed the effect of hAdSC transplantation with or without SimNPs on myocardial tissue regeneration. Representative Masson's trichrome staining images revealed that among all the groups, *de novo* muscle-like granulation tissue in the infarct zone was present only in the SimNP-AdSC group (Fig. 3E). The damaged infarct zone myocardium was then examined quantitatively. Although the LV fibrosis area was not significantly reduced, the LV fibrosis length was significantly reduced and the wall thickness in the scarred area was significantly increased in the SimNP-AdSC group (Fig. 3F). Fluorescence immunohistochemical analyses indicated that both ILB4-positive capillaries and $\text{SM}\alpha$ -actin-positive arteriole were frequently observed in the ischemic infarct area core site of the SimNP-AdSC-treated group only (Fig. 4A) and that the number of ILB4-positive capillaries (Fig. 4B) was significantly increased in the ischemic border zone of the SimNP-AdSC-treated group (Fig. 4C). Apoptotic, terminal deoxynucleotidyl transferase-mediated deoxyuridine triphosphate nick-end labeling TUNEL-positive cardiac cells were frequently observed in the control group but not in other

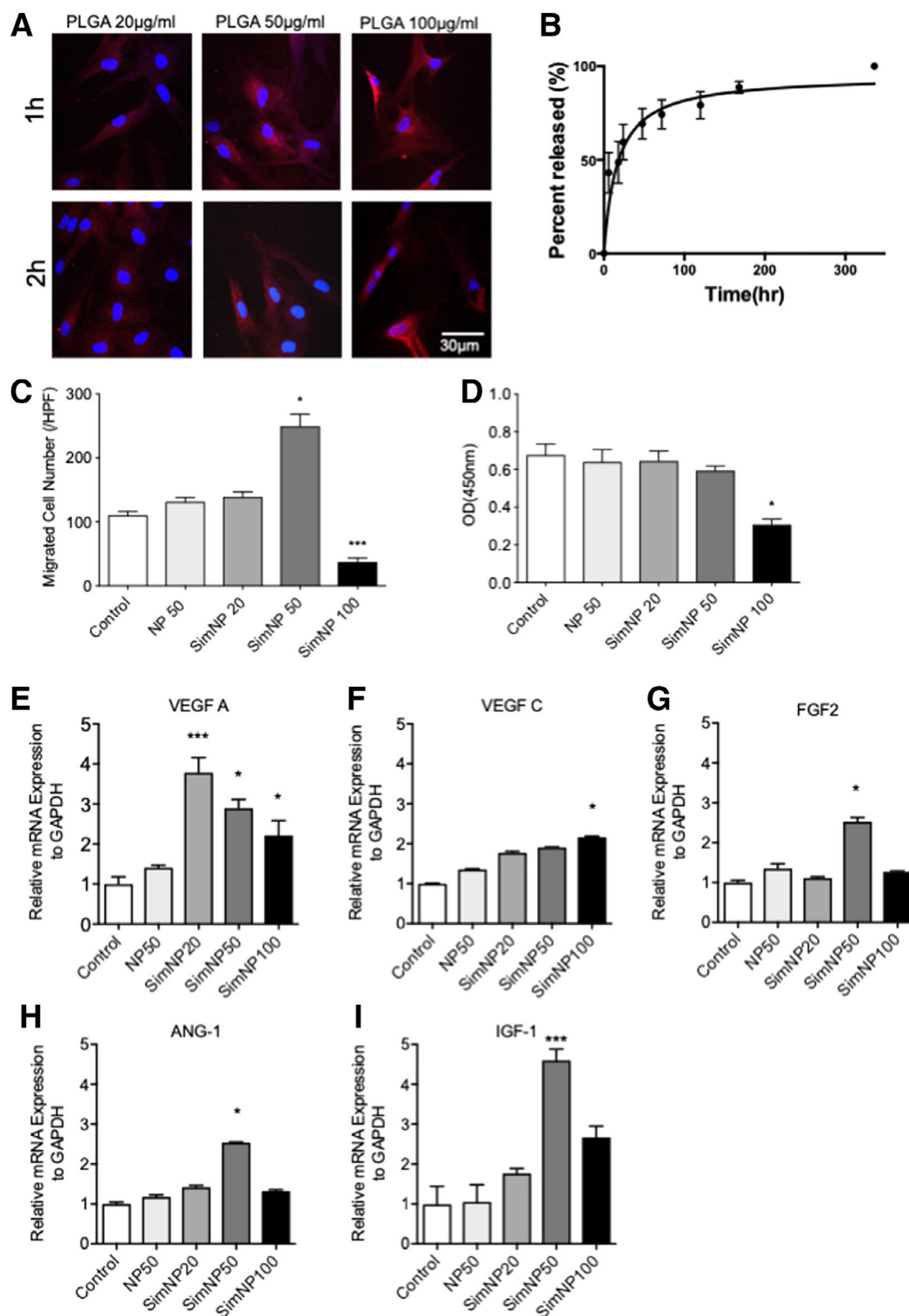


Figure 1. Proliferation and migration activities of human adipose-derived stem cells (hAdSCs) and poly(lactic-co-glycolic) acid (PLGA) nanoparticle (NP) uptake in hAdSCs. **(A):** The uptake of rhodamine-labeled (red) PLGA NPs in AdSCs was observed by confocal laser microscopy. **(B):** The in vitro time course of cumulative simvastatin release from AdSCs with the simvastatin-conjugated NPs (SimNPs; $n = 3$ in each time point). **(C):** The migration induced by 20% fetal bovine serum (FBS) was assessed by counting the number of migrated cells in a Transwell system after 6 hours of culturing ($n = 3$ in each group). **(D):** Proliferation activity was assessed by the 3-(4,5-dimethylthiazol-2-yl)-5-(3-carboxymethoxyphenyl)-2-(4-sulfophenyl)-2H-tetrazolium, inner salt MTS assay after 48 hours in culture with 10% FBS-containing medium ($n = 3$ in each group). **(E–I):** Quantitative real-time RT-PCR analyses for cytokine expression levels in hAdSCs ($n = 3$ in each group). The mRNA expression levels of vascular endothelial growth factor A (VEGF A; E), vascular endothelial growth factor C (VEGF C; F), basic fibroblast growth factor 2 (FGF 2; G), angiopoietin-1 (Ang-1; H), and insulin-like growth factor-1 (IGF-1; I) were assessed. Relative mRNA expression levels of the indicated cytokine genes were normalized to the GAPDH mRNA level and are presented in the graph. (*, $p < .05$; ***, $p < .001$ vs. control).

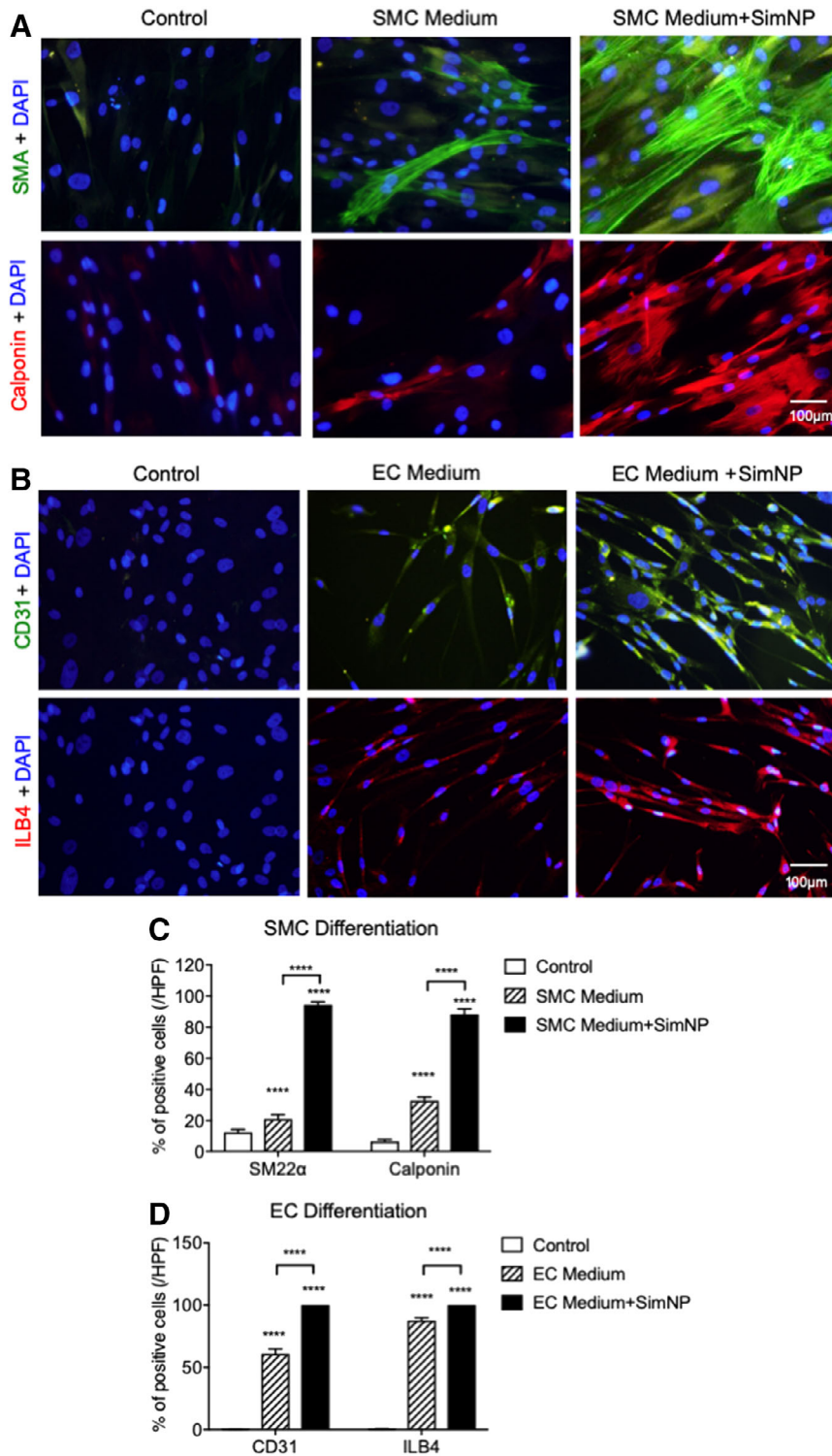


Figure 2. Fluorescence immunocytochemistry for adipose-derived stem cell (AdSC) endothelial and smooth muscle cell differentiation. **(A):** Human AdSCs (hAdSCs) were cultured with Dulbecco's modified Eagle medium (DMEM)/F12 medium (control), SMC differentiation medium (DMEM/F12 + TGF β 2 ng/ml), or SMC differentiation medium + SimNPs for 2 weeks. hAdSCs were positive for SM α -actin and Calponin expression under SMC medium culturing. To assess smooth muscle cell differentiation, the cells were stained with anti-SM α -actin (SMA, green) and anti-Calponin (red) antibodies. The nuclei were stained with DAPI (blue). **(B):** hAdSCs were cultured with DMEM/F12 medium (control), endothelial cell differentiation medium (EC medium), or EC medium + SimNPs for 2 weeks. To assess EC differentiation, the cells were stained with anti-ILB4 (green) and anti-CD31 (red) antibodies. The nuclei were stained with DAPI (blue). **(C):** The percentage of SM α -actin and Calponin-positive cells was compared among the three groups. **(D):** The percentage of CD31 and ILB4-positive cells was compared among the three groups. All experiments were performed in triplicate and analyzed statistically (****, $p < .0001$ vs. control, $n = 3$ in each group).

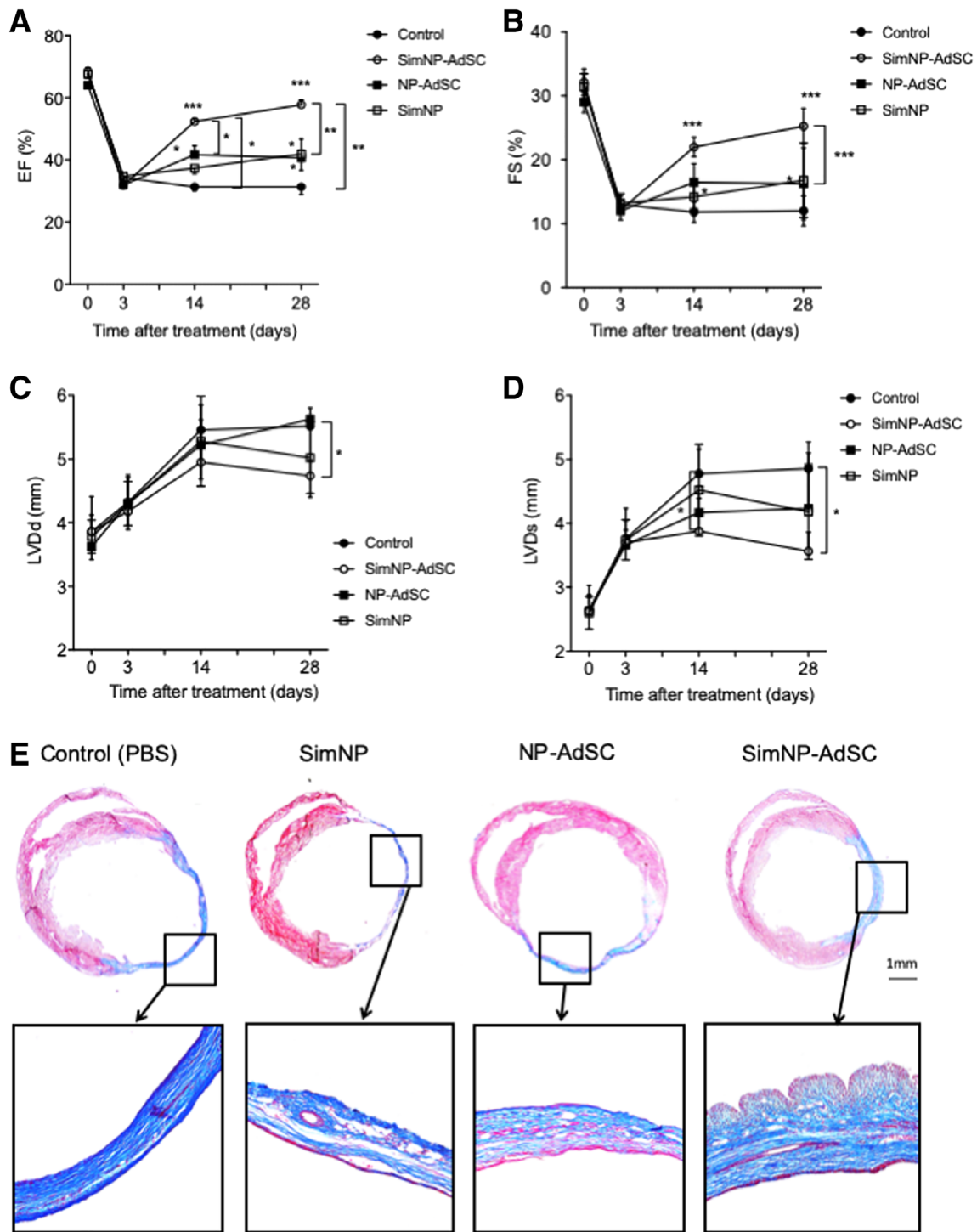


Figure 3. (Continued on next page).

groups. In contrast, quantitative analyses demonstrated that the percentage of TUNEL-positive cardiac cells was significantly reduced in the NP-AdSC and SimNP-AdSC groups compared with the control group (Fig. 4D). These results suggest that SimNP-AdSC transplantation preserved the global and regional LV function, with the reduced infarct size promoting neovascularization and inhibiting cell apoptosis in the ischemic myocardium after MI.

Recruited SimNP-AdSCs Induced Endogenous Cardiac Granulation Tissue Development in Infarcted Heart Tissue

First, at 3 days after cell infusion via the tail vein, we confirmed that human AdSCs (hAdSCs) were recruited to the ischemic myocardium. Double fluorescent detection for cardiac troponin-I (cTn-I), which is a marker for mature CMs (green), and rhodamine-conjugated PLGA NP-loaded hAdSCs (red) indicated that

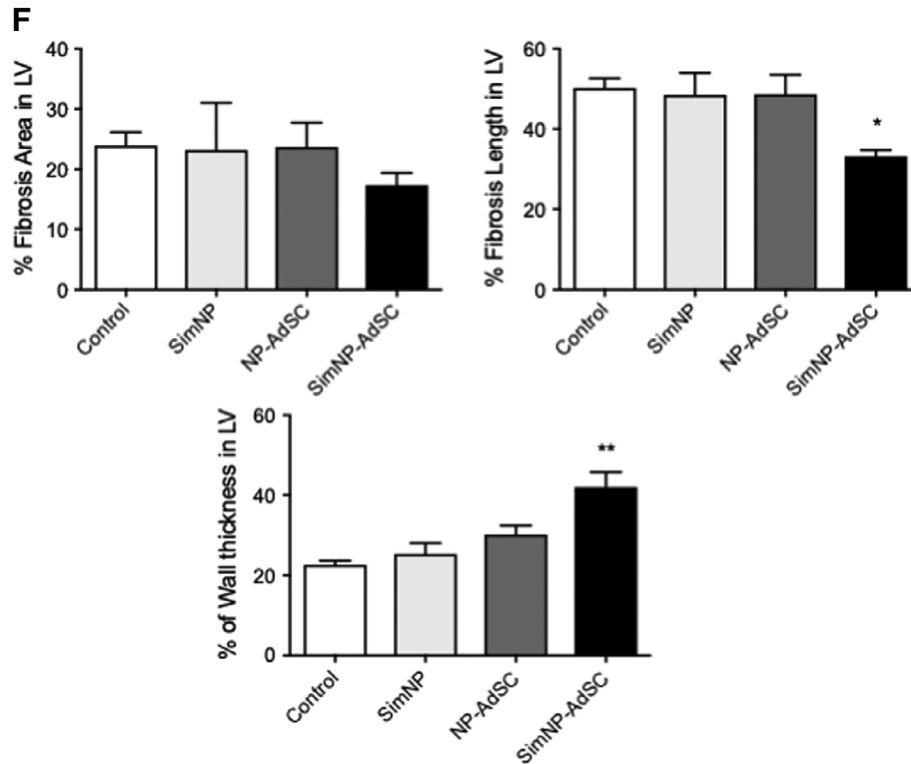


Figure 3. Echocardiographic and morphological assessment of cardiac function following the myocardial infarction surgery and treatments. The cardiac functional parameters (A) ejection fraction, (B) fractional shortening, (C) left ventricular end-diastolic dimension, and (D) left ventricular end-systolic dimension before the surgery and at 3, 14, and 28 days after the surgery were measured, and each parameter was analyzed statistically (*, $p < .05$; **, $p < .01$; ***, $p < .001$; and ****, $p < .0001$ vs. control, $n = 8$ in each group). Representative cardiac cross-sections of the infarcted myocardium at 28 days after surgery (E) in the control (phosphate buffered solution [PBS]) group, simvastatin-conjugated nanoparticle (SimNP; $10 \mu\text{g}$) group, NP-adipose-derived stem cell (AdSC; 10^4) group, and SimNP-AdSC ($10 \mu\text{g}/10^4$) group were assessed by Masson's trichrome staining. (F): The percentage of the left ventricle (LV) fibrosis area, LV fibrosis length, and LV wall thickness were measured in each group (*, $p < .05$; **, $p < .01$ vs. control, $n = 8$ in each group).

the systemically infused hAdSCs were recruited to the ischemic/damaged myocardium (Supporting Information Fig. S1). Next, to determine whether the recruited hAdSCs remained in the ischemic myocardium and transdifferentiated into CMs, we examined the hAdSCs by double immunofluorescence staining human mitochondria (hMitC) and cTn-I for CM. In the MI mice of the SimNP-AdSC ($10,000$ cells per mouse) group, no hMitC-positive cells were detected in the ischemic/damaged myocardium including in the de novo granulation tissue of the infarct area (data not shown). We then increased the number of SimNP-AdSCs for treatment to $50,000$ cells per mouse and examined the MI heart sections 28 days following surgery to check if some SimNP-AdSCs remained in the ischemic/damaged myocardium. A small number of cTn-I and hMitC double-positive cells were observed in the de novo granulation tissue (Supporting Information Fig. S2A), suggesting that a certain subpopulation of the transplanted SimNP-AdSCs survived and transdifferentiated into CMs in the ischemic myocardium.

We further characterized the granulation tissue in the infarct scarred area of the SimNP-AdSC group. Nkx2.5 and Gata4, indicated in green, are markers of immature CMs, and cardiac α myosin heavy chain (α MHC) and cTn-I, indicated in red, are markers of mature CM (Fig. 5A and Supporting Information Fig. S2B). On day 28 following the MI, a number of Nkx2.5-positive cells (Fig. 5A) and Gata4-positive cells (Supporting

Information Fig. S2B) were observed, whereas only a small number of α MHC-positive cells (Fig. 5A) and cTn-I-positive cells (Supporting Information Fig. S2B) were observed in the same area of the newly developed granulation tissue. Interestingly, a number of Wilms' tumor protein 1 (WT1)-positive cells were frequently detected in the ischemic myocardium 14 days following MI. WT1, which is expressed in the myocardium only during the fetal period, is transiently expressed on days 3–5 after the MI in C57B6/J mice. Indeed, regardless of the mouse strain (BALB/c, BALB/c nu/nu, C57B6/J), we detected no WT1 expression on postinfarction day 14. However, numerous WT1-positive cells were observed in the epicardial site of the infarcted myocardium in the SimNP-AdSC group, even on postinfarction day 14 (Supporting Information Fig. S3). WT1/Ki67 double-positive cells were also detected in the epicardial site of the ischemic/damaged myocardium, suggesting that the WT1-positive, proliferating epicardium-derived cells developed granulation tissue and perhaps differentiated into CMs (Fig. 5B).

Massive Myocardial Regeneration Was Induced by SimNP-AdSCs in the Scarred Infarct Area

Representative Masson's trichrome staining images revealed that even on day 56 following the MI, the PBS-treated heart still presented with a scarred infarcted myocardium. In contrast, in the SimNP-AdSC-treated heart, the scarred infarcted

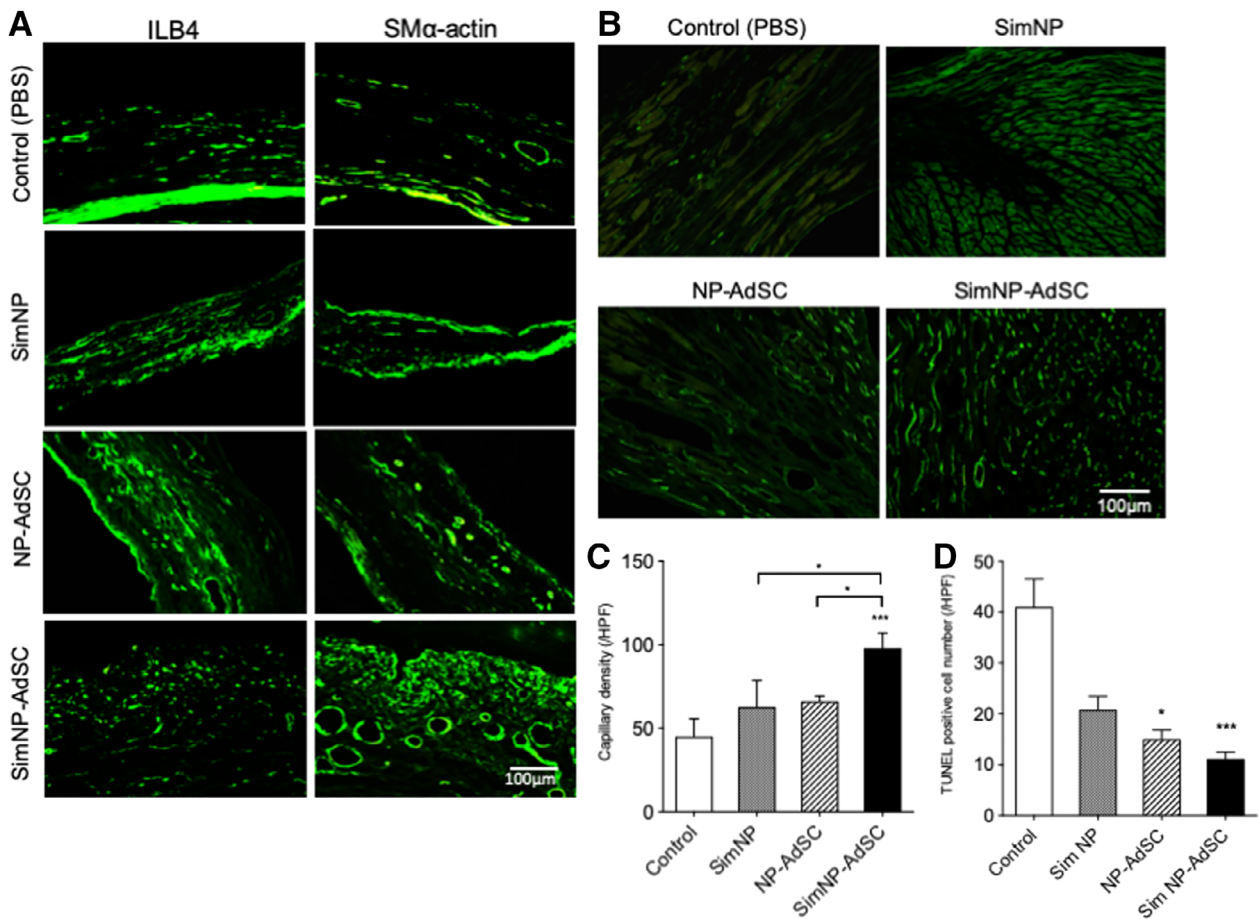


Figure 4. Immunohistological assessment of myocardial neovascularization and cardiac apoptosis in ischemic myocardium. **(A):** Representative cardiac cross-sections of the infarcted myocardium with Masson's trichrome staining at 28 days after surgery in the control (phosphate buffered solution [PBS]), simvastatin-conjugated nanoparticle (SimNP), NP-adipose-derived stem cell (AdSC), and SimNP-AdSC groups stained with Isolectin B4 (ILB4), an endothelial cell marker, and SM α -actin, a smooth muscle cell marker. **(B):** ILB4 staining for capillaries (green) in the ischemic border zone. **(C):** The capillary density in each group was calculated and is expressed in the graph. **(D):** Cardiac cell apoptosis was assessed by counting the number of TUNEL-positive cells in the ischemic core site of each group (*, $p < .05$; ***, $p < .001$ vs. control; $n = 8$ in each group).

myocardium with granulation tissue, which was observed on day 28 following MI, was largely replaced with regenerated de novo myocardium on day 56 (Fig. 6A). The damaged infarct zone myocardium was then examined quantitatively. The LV fibrosis area and length were significantly reduced and the wall thickness in the scarred area was significantly increased in the SimNP-AdSC group (Fig. 6B). The dramatic endogenous myocardial regeneration was also observed in another case in the SimNP-AdSC group (data not shown).

DISCUSSION

Marc Hedrick et al. were the first to isolate and identify adhesive pluripotent stem cells from adipose tissue in 2001 [22], and since then, research on adipose-derived stem cells (AdSCs) has rapidly advanced. AdSCs have attracted attention for clinical applications since fat tissue can be harvested easily and safely, and AdSCs can also be isolated and compared with other cell sources such as BM-derived stem cells. AdSCs effectiveness has often been reported in MI animal models. Moreover, clinical trials have recently reported the safety and therapeutic effect of

AdSCs on chronic myocardial ischemia and acute MI in Europe and the U.S. [23, 24]. However, a large number of AdSCs are required for a sufficient therapeutic effect. Considering these clinical applications, harvesting large numbers of cells from patients who are elderly or who have underlying diseases such as diabetes is often difficult and decreased cell-trophic effects have also been reported [25, 26]. For these reasons, the favorable outcomes of AdSC treatment alone may be limited. Thus, we were challenged to explore a novel strategy to increase the therapeutic potential of even a small number of AdSCs with "statins" for transplantation.

Statins are known to have pleiotropic effects in addition to their serum lipid-lowering ability and improve collateral circulation in the ischemic heart [27] and ischemic limbs [28, 29] in animal studies. However, these pro-angiogenic effects often require high daily systemic doses, which may lead to adverse effects in actual clinical practice. Therefore, we focused on bioabsorbable polymer (PLGA)-nanoparticles (NPs; PLGA-NPs) as an ideal material for local statin delivery and tested the hypothesis that the combination of statin-PLGA-NPs and AdSCs synergistically exhibit a favorable effect in a mouse model of MI. Improved cardiac function and a reduced infarct site area

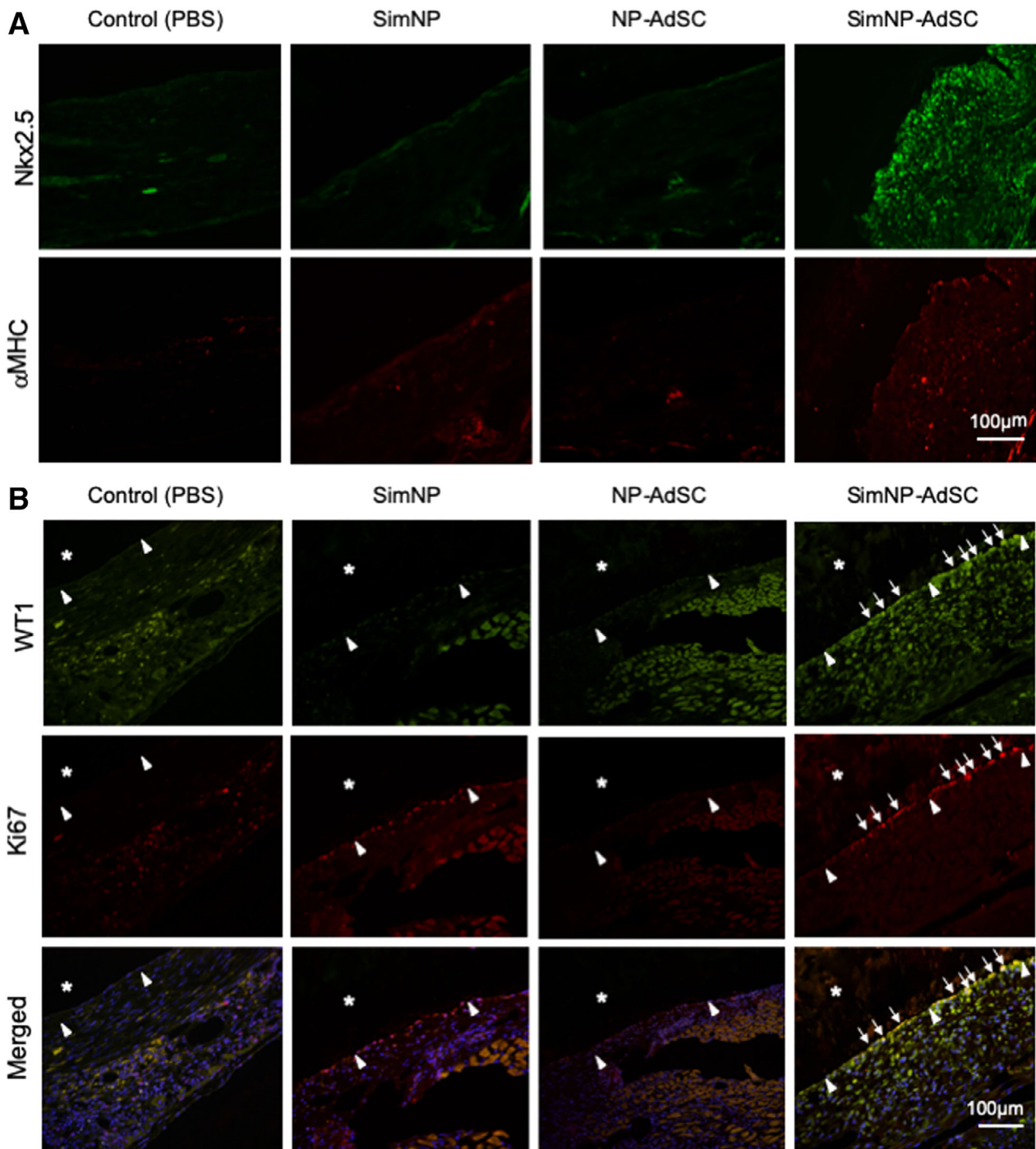


Figure 5. Fluorescence immunostaining of the ischemic myocardium with de novo tissue granulation. **(A):** Cross-sections from infarcted myocardium with Masson's trichrome staining at 28 days after surgery in the control (phosphate buffered solution [PBS]) group, simvastatin-conjugated nanoparticle (SimNP; 10 μ g) group, NP-adipose-derived stem cell (AdSC; 10^4) group, and SimNP-AdSC (10 μ g/ 10^4) group stained with Nkx2.5, a marker for immature cardiomyocytes, as indicated in green, and cardiac alpha myosin heavy chain (α MHC), a marker for mature cardiomyocyte, in red. **(B):** Double fluorescent immunostaining for WT1 (Wilms' tumor protein 1; green) and Ki67 (red) expression in the ischemic core site of the control (PBS) group, SimNP (10 μ g) group, NP-AdSC (10^4) group, and SimNP-AdSC (10 μ g/ 10^4) group at 14 days after surgery ($n = 3$ in each group). *, outer side of heart; arrowheads, epicardium; and arrows, WT1/Ki67 double-positive cells.

were observed only in the group treated with a combination of statin-loaded PLGA-NPs (SimNPs) and AdSCs. With SimNPs alone or with AdSCs combined with nondrug containing PLGA-NPs, no therapeutic effect was observed. The reason for the lack of therapeutic effect with the SimNPs alone was probably

because the nanoparticles themselves did not sufficiently accumulate within the infarct site. Additionally, the combined AdSC and nondrug containing PLGA-NP treatment failed to activate cell function, and the number of cells was too small to achieve effectiveness with AdSCs alone. Following quick (within

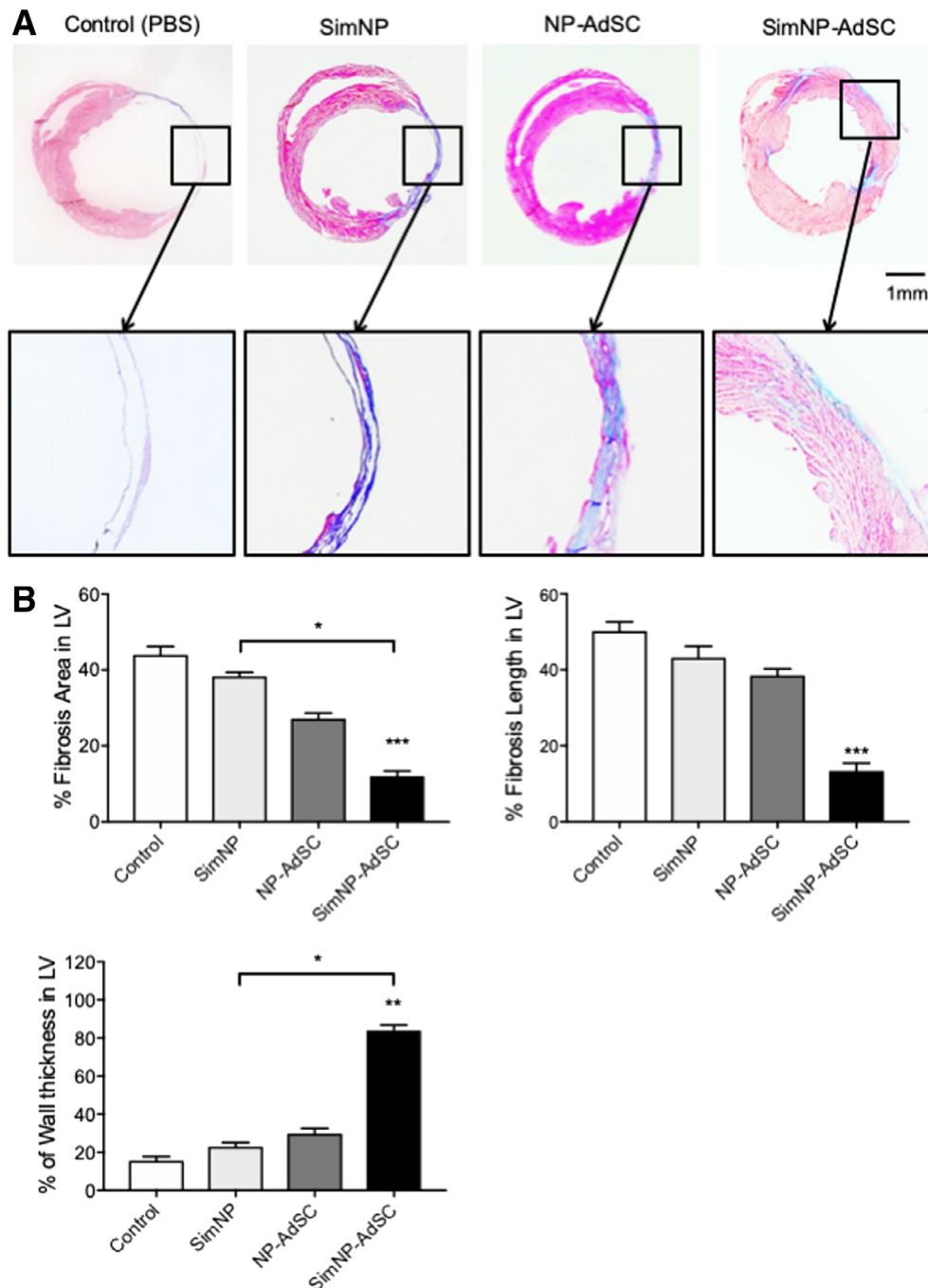


Figure 6. Histology in the myocardium at 56 days after the myocardial infarction surgery and treatments. The hearts were histologically assessed by Masson's trichrome staining at a cross-sectional level of 1 mm below left anterior descending ligation/suture level (**A**) in the control (phosphate buffered solution) group, simvastatin-conjugated nanoparticle (SimNP; 10 μ g) group, NP-adipose-derived stem cell (AdSC; 10^4) group, and SimNP-AdSC (10 μ g/ 10^4) group at 56 days after surgery. (**B**): The percentage of the left ventricle (LV) fibrosis area, LV fibrosis length, and LV wall thickness were measured in each group (**, $p < .01$; ***, $p < .001$ vs. control; $n = 3$ in each group).

1 hour) AdSC uptake of the statin-encapsulated PLGA-NPs, since the recruitment of transplanted AdSCs to ischemic myocardium would be also rapid, perhaps within a couple of hours, most of the loaded NPs will be still inside the AdSCs and significant amount of SimNPs would therefore be delivered to the ischemic myocardium. The recruited AdSCs released statin slowly along with intracellular PLGA hydrolysis and the statin promoted

AdSC migration activity peaking at a dose of 50 μ g/50,000 cells SimNP but inhibiting at a dose of 100 μ g/50,000 cells SimNP. The inhibitory effect of SimNP at a dose of 100 μ g/50,000 cells was attributed to over loading of PPGA-NPs on AdSCs or high dose of statin exposure to AdSCs, since high dose of statin is known to have an inhibitory effect on endothelial cell migration [30].

We detected the accumulation of rhodamine-labeled SimNPs in cardiac tissue (Supporting Information Fig. S1B). We then speculate the reason why SimNP group demonstrated little therapeutic effect on myocardial tissue regeneration is because of insufficient concentration of simvastatin in local tissue. A systemically administered, small number of statin-PLGA-NP-loaded AdSCs were significantly recruited to the ischemic myocardium, and then, the statin was locally gradually released for cardiac tissue regeneration. AdSCs appear to play a role as a bio-DDS for sustained statin release at MI sites only (Supporting Information Fig. 4). The sustained statin release from the recruited AdSCs might not only inhibit tissue inflammation [31] but also promote of circulating BM-derived stem/progenitor cell recruitment, contributing to enhanced angiogenesis in the ischemic myocardium [32–34]. Furthermore, locally released statin might activate WT1-positive, epicardium-derived cells [35], and resident cardiac stem/progenitor cells and promote the transdifferentiation of these cells into CMs.

The therapeutic effect in our study was achieved with a smaller number of AdSCs than has ever been reported [19, 36] (Supporting Information Table S1). These functionally enhanced AdSCs with encapsulated statin-PLGA-NPs accumulated in the ischemic myocardium, and localized, sustained statin release from the AdSCs enhanced the effectiveness of epicardial cell-derived myocardial tissue regeneration, since no AdSCs remained or were differentiated into vascular endothelial cells (ECs), vascular smooth muscle cells (VSMCs), and myocardial cells in the regenerated myocardium (data not shown). The effects of locally released-statins in SimNP-AdSC group rather than the recruited AdSCs in NP-AdSC group appear to contribute to significant cardiac functional recovery with intrinsic myocardial tissue regeneration. This evolutionary technology may lead to the next generation of stem cell therapy not only for MI but also for other type of diseases, specifically inflammatory diseases. Indeed, we have already confirmed that this therapeutic strategy was fairly effective in autoimmune diseases such as interstitial pneumonia, scleroderma, and ulcerative colitis.

CONCLUSION

This unique method allows us to reduce the number of stem cells required for transplantation, allowing pulmonary thromboembolism to be avoided as a complication and reducing the amount of

medicine may also avoid adverse side effects. Several promising features of this method exist: AdSC NP treatment (a) has a low-cost due to using somatic stem cells and the clinically available, established medicine statin; (b) is a quick and easy therapy due to the simple AdSC isolation procedure with rapid PLGA-NP uptake in AdSCs and the administration of intravenous drip infusions; and (c) sufficiently facilitates endogenous functional cardiac regeneration, which can avoid unnecessary/aggressive coronary interventional therapy or open-chest cardiac bypass surgery, resulting in a large reduction in medical expenses. We believe the practical use of this therapeutic strategy will provide relief for humans suffering from incurable diseases. An international patent application (PCT/JP2015/081329) aiming to clinically apply this technology has been filed, and a Japanese patent based on the PCT/JP2015/081329 patent application was issued in March 2017.

ACKNOWLEDGMENT

This work was supported by Japan Society for the Promotion of Science KAKENHI grant number JP16K08562.

AUTHOR CONTRIBUTIONS

R.Y.: collection and assembly of data, data analysis and interpretation, manuscript writing, final approval of manuscript; M.I.: conception and design, manuscript writing, collection and assembly of data, data analysis and interpretation, final approval of manuscript; M.M.: collection and assembly of data; Y.T.: provision of study material, data analysis and interpretation, final approval of manuscript; M.H., N.I., M.A.: data analysis and interpretation, final approval of manuscript.

DISCLOSURE OF POTENTIAL CONFLICTS OF INTEREST

The authors indicated no potential conflicts of interest.

DATA AVAILABILITY STATEMENT

The data that support the findings of this study are available from the corresponding author upon reasonable request.

REFERENCES

- Guilbert JJ. The world health report 2002—Reducing risks, promoting healthy life. *Educ Health* 2003;16:230.
- Losordo DW, Schatz RA, White CJ et al. Intramyocardial transplantation of autologous CD34+ stem cells for intractable angina: A phase I/IIa double-blind, randomized controlled trial. *Circulation* 2007;115:3165–3172.
- Ghodsizad A, Niehaus M, Kogler G et al. Transplanted human cord blood-derived unrestricted somatic stem cells improve left-ventricular function and prevent left-ventricular dilation and scar formation after acute myocardial infarction. *Heart* 2009;95:27–35.
- Miyahara Y, Nagaya N, Kataoka M et al. Monolayered mesenchymal stem cells repair scarred myocardium after myocardial infarction. *Nat Med* 2006;12:459–465.
- Li TS, Hayashi M, Ito H et al. Regeneration of infarcted myocardium by intramyocardial implantation of ex vivo transforming growth factor-beta-preprogrammed bone marrow stem cells. *Circulation* 2005;111:2438–2445.
- Planat-Benard V, Silvestre JS, Cousin B et al. Plasticity of human adipose lineage cells toward endothelial cells: Physiological and therapeutic perspectives. *Circulation* 2004;109:656–663.
- Rehman J, Traktuev D, Li J et al. Secretion of angiogenic and antiapoptotic factors by human adipose stromal cells. *Circulation* 2004;109:1292–1298.
- Planat-Benard V, Menard C, Andre M et al. Spontaneous cardiomyocyte differentiation from adipose tissue stroma cells. *Circ Res* 2004;94:223–229.
- Jumabay M, Zhang R, Yao Y et al. Spontaneously beating cardiomyocytes derived from white mature adipocytes. *Cardiovasc Res* 2010;85:17–27.
- Nagata H, Li M, Kohbayashi E et al. Cardiac adipose-derived stem cells exhibit high differentiation potential to cardiovascular cells in C57BL/6 mice. *STEM CELLS TRANSLATIONAL MEDICINE* 2016;5:141–151.
- Li M, Horii M, Yokoyama A et al. Synergistic effect of adipose-derived stem cell therapy and bone marrow progenitor recruitment in ischemic heart. *Lab Invest* 2011;91:539–552.
- Mazo M, Planat-Benard V, Abizanda G et al. Transplantation of adipose derived stromal cells is associated with functional improvement in a rat model of chronic myocardial infarction. *Eur J Heart Fail* 2008;10:454–462.

- 13** Cai L, Johnstone BH, Cook TG et al. IFATS collection: Human adipose tissue-derived stem cells induce angiogenesis and nerve sprouting following myocardial infarction, in conjunction with potent preservation of cardiac function. *STEM CELLS* 2009;27:230–237.
- 14** Cai A, Zheng D, Dong Y et al. Efficacy of Atorvastatin combined with adipose-derived mesenchymal stem cell transplantation on cardiac function in rats with acute myocardial infarction. *Acta Biochim Biophys Sin* 2011;43:857–866.
- 15** Katsuki S, Matoba T, Nakashiro S et al. Nanoparticle-mediated delivery of pitavastatin inhibits atherosclerotic plaque destabilization/rupture in mice by regulating the recruitment of inflammatory monocytes. *Circulation* 2014;129:896–906.
- 16** Matoba T, Egashira K. Nanoparticle-mediated drug delivery system for cardiovascular disease. *Int Heart J* 2014;55:281–286.
- 17** Ii M, Losordo DW. Statins and the endothelium. *Vascul Pharmacol* 2007;46:1–9.
- 18** Yang YJ, Qian HY, Huang J et al. Atorvastatin treatment improves survival and effects of implanted mesenchymal stem cells in post-infarct swine hearts. *Eur Heart J* 2008;29:1578–1590.
- 19** Bai X, Yan Y, Song YH et al. Both cultured and freshly isolated adipose tissue-derived stem cells enhance cardiac function after acute myocardial infarction. *Eur Heart J* 2010;31:489–501.
- 20** Ii M, Nishimura H, Iwakura A et al. Endothelial progenitor cells are rapidly recruited to myocardium and mediate protective effect of ischemic preconditioning via “imported” nitric oxide synthase activity. *Circulation* 2005;111:1114–1120.
- 21** Iwasaki H, Kawamoto A, Ishikawa M et al. Dose-dependent contribution of CD34-positive cell transplantation to concurrent vasculogenesis and cardiomyogenesis for functional regenerative recovery after myocardial infarction. *Circulation* 2006;113:1311–1325.
- 22** Zuk PA, Zhu M, Ashjian P et al. Human adipose tissue is a source of multipotent stem cells. *Mol Biol Cell* 2002;13:4279–4295.
- 23** Houtgraaf JH, den Dekker WK, van Dalen BM et al. First experience in humans using adipose tissue-derived regenerative cells in the treatment of patients with ST-segment elevation myocardial infarction. *J Am Coll Cardiol* 2012;59:539–540.
- 24** Perin EC, Sanz-Ruiz R, Sanchez PL et al. Adipose-derived regenerative cells in patients with ischemic cardiomyopathy: The PRECISE trial. *Am Heart J* 2014;168:88.e2–95.e2.
- 25** Efimenko A, Dzhyoyashvili N, Kalinina N et al. Adipose-derived mesenchymal stromal cells from aged patients with coronary artery disease keep mesenchymal stromal cell properties but exhibit characteristics of aging and have impaired angiogenic potential. *STEM CELLS TRANSLATIONAL MEDICINE* 2014;3:32–41.
- 26** Dzhyoyashvili NA, Efimenko AY, Kochegura TN et al. Disturbed angiogenic activity of adipose-derived stromal cells obtained from patients with coronary artery disease and diabetes mellitus type 2. *J Transl Med* 2014;12:337.
- 27** Landmesser U, Engberding N, Bahlmann FH et al. Statin-induced improvement of endothelial progenitor cell mobilization, myocardial neovascularization, left ventricular function, and survival after experimental myocardial infarction requires endothelial nitric oxide synthase. *Circulation* 2004;110:1933–1939.
- 28** Sata M, Nishimatsu H, Suzuki E et al. Endothelial nitric oxide synthase is essential for the HMG-CoA reductase inhibitor cerivastatin to promote collateral growth in response to ischemia. *FASEB J* 2001;15:2530–2532.
- 29** Kureishi Y, Luo Z, Shiojima I et al. The HMG-CoA reductase inhibitor simvastatin activates the protein kinase Akt and promotes angiogenesis in normocholesterolemic animals. *Nat Med* 2000;6:1004–1010.
- 30** Skaletz-Rorowski A, Walsh K. Statin therapy and angiogenesis. *Curr Opin Lipidol* 2003;14:599–603.
- 31** Jain MK, Ridker PM. Anti-inflammatory effects of statins: Clinical evidence and basic mechanisms. *Nat Rev Drug Discov* 2005;4:977–987.
- 32** Dimmeler S, Aicher A, Vasa M et al. HMG-CoA reductase inhibitors (statins) increase endothelial progenitor cells via the PI 3-kinase/Akt pathway. *J Clin Invest* 2001;108:391–397.
- 33** Llevadot J, Murasawa S, Kureishi Y et al. HMG-CoA reductase inhibitor mobilizes bone marrow-derived endothelial progenitor cells. *J Clin Invest* 2001;108:399–405.
- 34** Urbich C, Dernbach E, Zeiher AM et al. Double-edged role of statins in angiogenesis signaling. *Circ Res* 2002;90:737–744.
- 35** van Wijk B, Gunst QD, Moorman AF et al. Cardiac regeneration from activated epicardium. *PLoS One* 2012;7:e44692.
- 36** Bai X, Alt E. Myocardial regeneration potential of adipose tissue-derived stem cells. *Biochem Biophys Res Commun* 2010;401:321–326.



See www.StemCellsTM.com for supporting information available online.